Cancer Research

Identification of a Molecular Signature Underlying Inhibition of Mammary Carcinoma Growth by Dietary N-3 Fatty Acids

Weiqin Jiang[1], Zongjian Zhu[1], John N. McGinley[1], Karam El Bayoumy[2], Andrea Manni[2], and Henry J. Thompson[1]

Abstract

An increased ratio of dietary n-3 relative to n-6 fatty acids has been shown to inhibit the development of mammary cancer in animal models. However, the molecular mechanisms by which n-3 fatty acids affect tumor growth remain unknown. Here, we investigated the effects of varying dietary ratios of n-3:n-6 fatty acids on cell signaling in a rat model of chemically induced mammary carcinoma. Cell proliferation was reduced by 60% in carcinomas from the high n-3:n-6 treatment group compared with the low n-3:n-6 treatment group. These changes were associated with decreased cyclin-D1 and phospho-retinoblastoma protein expression and increased levels of cyclin-dependent kinase inhibitors, CIP1 (p21) and KIP1 (p27). In addition, the apoptotic index was increased in carcinomas from the high n-3:n-6 group and was associated with elevated apoptotic protease-activating factor 1 and a higher ratio of Bax/Bcl-2. Interestingly, changes in protein expression were consistent with reduced inflammation and suppressed mTOR activity, and the molecular signature associated with high n-3:n-6 treatment revealed changes in PPARγ activation and suppression of lipid synthesis. Together, our findings indicate that the molecular effects of high dietary n-3 to n-6 ratios are heterogeneous in nature but point to consistent changes in lipid metabolism pathways, which may serve as potential therapeutic targets for cancer prevention and control. This study identifies the pathways modulated by dietary fatty acid ratios in a rat model of breast cancer, with implications for cancer prevention. *Cancer Res; 72(15); 3795–806. ©2012 AACR.*

Introduction

Previous work identified dietary concentrations of n-3 relative to n-6 fatty acids that inhibited chemically induced mammary carcinogenesis (1). Of the various aspects of the carcinogenic response inhibited, the effect of high n-3:n-6 was greatest on tumor burden. Because an understanding of the mechanisms by which n-3 fatty acids affect the balance between cell proliferation and cell death is important to assess their potential value in both cancer prevention and cancer control (2), this investigation focused on identifying candidate pathways by which a high dietary ratio of n-3:n-6 affected tumor size homeostasis, that is, the balance between cell proliferation and cell death (3). There are many avenues through which dietary n-3:n-6 ratio could be exerting effects (1, 4), of which the activation of PPARs (5, 6) and the altered synthesis of types and/or amounts of tissue eicosanoids may be particularly relevant to carcinogenesis (7, 8, 9). While there are canonical patterns of cell signaling induced by PPAR activation (7), evidence continues to emerge implicating additional effects not directly linked to the transcriptional activity of n-3 fatty acids bound to their cognate receptors (10). Moreover, eicosanoids themselves may exert effects on tumor growth that parallel those of PPARs but via mechanisms independent of PPAR activation (9). Thus, rather than focus on one specific aspect of n-3 fatty acid molecular biology, our goal was to explore pathways implicated by our previous report (1) on the effects of the dietary n-3:n-6 fatty acid ratio on host systemic factors under circumstances in which a profound effect on tumor growth rate was observed.

The data reported indicate that canonical pathways associated with n-3 fatty acid activation of PPARs as well as noncanonical pathways involving components of mTOR signaling mediate effects on intratumoral lipid biosynthesis as a potential mechanism by which tumor growth is limited.

Materials and Methods

Chemicals and reagents

Concentrated ϖ-3 oil was purchased from American International Chemical, Inc. All experimental diets were purchased from Research Diets. *N*-Methyl-*N*-nitrosourea (MNU; Ash Stevens) was stored at −80°C before use. Primary antibodies used in this study were anti-cyclin-D1, anti-p27^{Kip1}, and anti-Ki-67 (clone SP6) from Thermo Fisher Scientific; anti-Bax and anti-Bcl-2 from BD Biosciences (anti-GADD153, Hif-1α, and GPR120 from Novus Biologicals, anti-pIRS/pIRS, anti-PARPs,

Authors' Affiliations: [1]Cancer Prevention Laboratory, Colorado State University, Fort Collins, Colorado; and [2]Penn State University College of Medicine, Hershey, Pennsylvania

Note: Supplementary data for this article are available at Cancer Research Online (http://cancerres.aacrjournals.org/).

Corresponding Author: Henry J. Thompson, Cancer Prevention Laboratory, Colorado State University, 1173 Campus Delivery, Fort Collins, CO 80523. Phone: 970-491-7748; Fax: 970-491-3542; E-mail: henry.thompson@colostate.edu

doi: 10.1158/0008-5472.CAN-12-1047

anti-pRB/RB, anti-Apaf-1, anti-pFOXO1&3/FOXO1&3, anti-NFkB-p65, anti-SIRT-1, anti-FASN, anti-PI3Kp110, anti-pAMPK/AMPK, anti-pACC/ACC, anti-pAkt/Akt, anti-pmTOR/mTOR, anti-pP70S6/P70S6, anti-p4E-BP1/4E-BP1, anti-p-Raptor/Raptor, anti-p-PRAS40/PRAS40, anti-rabbit immunoglobulin-horseradish peroxidase (HRP)-conjugated secondary antibody, and LumiGLO reagent with peroxide were purchased from Cell Signaling Technology; anti-IGFR-1, anti-p21^{Cip1}, anti-PPARα, β, γ, anti-HMGCR, anti-SREBP-1, and anti-mouse immunoglobulin-HRP-conjugated secondary antibody were from Santa Cruz; and mouse anti-β-actin primary antibody was obtained from Sigma-Aldrich. Biotinylated donkey anti-rabbit, donkey anti-goat secondary antibodies, and normal donkey serum were obtained from Jackson ImmunoResearch; HRP-conjugated streptavidin was obtained from Dako; and stable 3,3′-diaminobenzidine was obtained from Invitrogen.

Animals and experimental design

The tissue evaluated in this study was from a previously reported experiment. Briefly, in that study, 21-day-old rats were injected with 50 mg MNU/kg body weight (intraperitoneally) as previously described (11). Seven days following carcinogen injection, all rats were randomized into treatment groups, 30 rats per group, and were fed their respective experimental diets. The actual fatty acid content of each diet was determined by gas chromatography-mass spectroscopy (GC-MS) as previously described (1), and the fatty acid data are shown in Supplementary Table S1. The rats were fed diets in which the ratio of n-3:n-6 was either 0.7 (low n-3, control) or 14.6 (high n-3). Diet and water were provided *ad libitum*. Rats were weighed weekly and palpated for detection of mammary tumors twice per week. Animal rooms were maintained at 22°C ± 1°C with 50% relative humidity and a 12-hour light/12-hour dark cycle. At necropsy, detectable mammary pathologies were excised and weighed. A section of each lesion was fixed in neutral-buffered formalin and prepared for histologic classification; the remainder of each lesion was snap-frozen in liquid nitrogen for molecular determination; only confirmed mammary carcinomas were used in this study. The work reported was reviewed and approved by the Institutional Animal Care and Use Committee and conducted according to the committee guidelines.

Determination of rates of cell proliferation and apoptosis

Ki-67 immunohistochemical staining was used as an index of tumor growth fraction and was determined as previously described (12). Ten representative images of each Ki-67–stained section were chosen at random and acquired using a Zeiss Axioskop II (Carl Zeiss, Inc.) at a magnification of ×400 and analyzed using Image Pro Plus 4.5 (Media Cybernetics, Inc.). Apoptosis was quantified using the criteria developed by Kerr for its detection (13, 14); 10 images of corresponding hematoxylin and eosin-stained serial sections were acquired at ×400. Apoptotic and normal cells were marked and counted using the count tool in Adobe Photoshop CS4 (Adobe Systems, Inc.). The apoptotic index was computed as the number of apoptotic cells divided by the total number of cells counted and was expressed as a percentage.

Western blotting

Twenty-two mammary carcinomas, each from a different rat (11 per group) were homogenized in lysis buffer [40 mmol/L Tris-HCl (pH 7.5), 1% Triton X-100, 0.25 mol/L sucrose, 3 mmol/L EGTA, 3 mmol/L EDTA, 50 μmol/L β-mercaptoethanol, 1 mmol/L phenylmethylsulfonyl fluoride, and complete protease inhibitor cocktail (Calbiochem)]. The lysates were centrifuged at 7,500 × *g* for 10 minutes at 4°C and supernatant fractions were collected and stored at −80°C. Supernatant protein concentrations were determined by the Bio-Rad Protein Assay (Bio-Rad). Western blotting was conducted as described previously (15). Briefly, 40 μg of protein lysate per sample was subjected to 8% to 16% SDS-PAGE after being denatured by boiling with SDS sample buffer [63 mmol/L Tris-HCl (pH 6.8), 2% SDS, 10% glycerol, 50 mmol/L dithiothreitol (DTT), and 0.01% bromophenol blue] for 5 minutes. After electrophoresis, proteins were transferred to a nitrocellulose membrane. The levels of IGF1R, pIRS, IRS, PI3Kp110, cyclin-D1, p27^{Kip1}, p21^{Cip1}, pRb, Rb, Bax, Bcl-2, Apaf-1, c-PARPs (PARP89 and PARP116), pAMPK, AMPK, pACC, ACC, HMGCR, SREBP-1 (precursor, not mature form), FASN, pAkt, Akt, pmTOR, mTOR, pP70S6, P70S6, p-4E-BP1, 4E-BP1, p-Raptor, Raptor, pPRAS40, PRAS40, PPARα, β, γ, GPR120, NFkBp65, pFOXO1&3a, FOXO1&3a, Hif-1α, SIRT-1, GADD153, and β-actin were determined using specific primary antibodies, followed by treatment with the appropriate peroxidase-conjugated secondary antibodies and visualized by LumiGLO reagent Western Blotting Detection System. The chemiluminescence signal was captured using a ChemiDoc densitometer (Bio-Rad) that was equipped with a CCD camera having a resolution of 1,300 × 1,030. Quantity One software (Bio-Rad) was used in the analysis. All of the Western blotting signals were within a range where the signal was linearly related to the mass of protein. The Quantity One software has a warning algorithm that notifies the user if pixel density is approaching saturation so that all signals used for analysis are in the linear range. The actin-normalized scanning density data were used for analysis.

Statistical analyses

Differences among groups in Ki-67 staining, apoptotic index, and the actin-normalized Western blot data were analyzed by the Kruskal–Wallis rank test as implemented in Systat version 13 (Systat Software, Inc.; ref. 16). All *P* values are 2-sided and statistical significance was set *a priori* at $P < 0.05$.

Soft independent modeling of class analogue analysis

Principal components analysis (PCA) is an unsupervised cluster analysis method for summarizing a set of correlated variables by transforming them, by means of an eigen decomposition, into a new set of uncorrelated variables, typically reducing the dimensionality of the original data set. The procedure is carried out with no prior knowledge of class membership. The first principal component (PC) is the linear combination of the features (actin-normalized scanning data from Western blotting) that passes through the centroid of the

full data set while minimizing the square of the perpendicular distance of each point to that line; each subsequent PC is constructed in a similar manner, subject to the constraint of being mutually orthogonal (17). The PCA model can be written as

$$X = Xbar + TP' + E \quad (A)$$

where X is the matrix of Western blotting values, *Xbar* is a vector of means (all 0 when the data are centered), T is a matrix of scores that summarize the X variables, P′ is a matrix of loadings, and E is a matrix of residuals.

Orthogonal projections to latent structures for discriminant analysis (OPLS-DA) is a supervised, class-based method where class membership is assigned and used to elicit maximum data separation (18–21). The OPLS-DA model can be written as

$$X = T_pP'_p + T_oP'_o + E \quad (B)$$

The interpretation of (B) is similar to that for the PCA model; however, an additional rotation has been applied using the class information to partition TP′ into a predictive, T_pP_p', and an orthogonal, T_oP_o', component. The number of predictive and orthogonal components in the models was determined by cross-validation. Three key statistics describe the fit of each model. First, R2X(cum) is the total amount of variation (predictive + orthogonal) explained in X; R2Y(cum) is the total amount of the variation explained in Y; and third, Q2Y(cum) is the total amount of predicted variability in Y (the goodness of prediction), estimated by 7-fold cross-validation. The contribution of each component partitioned into between (predictive) and within (orthogonal) class is also estimated and summarized as $R2X_p$ and $R2X_o$, respectively. $R2X_p$ and $R2X_o$ sum to R2X(cum). The ability of the model to classify the observations into the defined classes is reflected in misclassification rates for each model, where the target proteins of mammary carcinomas determined by Western blotting were classified on the basis of the modeled probability of a single observation belonging to a particular class.

All analyses were conducted using soft independent modeling of class analogue (SIMCA) analysis, SIMCA-P+ v.12.0.1 (Umetrics).

Results

Carcinogenic response

In the high versus low n-3:n-6 treatment groups, cancer incidence was reduced by 21%, cancer multiplicity by 30%, cancer mass by 79.9%, and cancer latency was prolonged by 15.8%. These effects were statistically significant as shown in Supplementary Table S2. The focus of the analyses reported herein was to investigate the mechanisms that accounted for the 79.9% reduction in tumor burden, as the reduction in tumor burden was clearly greater than could be accounted for by the effects of the high n-3 ratio in delaying cancer latency, which would decrease the length of time over which tumors grew. To that end, 11 carcinomas were analyzed from each group of the different animals. The carcinomas selected were non-necrotic, sufficiently large for an extended number of analyses, and representative of the differences in carcinoma mass and latency in the treatment groups from which the carcinomas were obtained (Supplementary Table S2). The values for the selected carcinomas evaluated herein were carcinoma mass, 2.56 ± 1.68 g versus 0.19 ± 0.13 g (mean $\pm$ SD; $P = 0.001$), time to detection, 37.5 [95% confidence interval (CI), 34.5–40.5] days and 44.3 (95% CI, 41.5–47.0; $P = 0.004$; Mantel test), respectively, for the low versus high n-3 treatment groups. Estimated tumor growth rates (mg/d) were 181 ± 70 and 48 ± 48 (mean $\pm$ SD, $P < 0.005$), respectively, for the low and high n-3:n-6 treatment groups.

Cell proliferation and death

To ascertain what cellular process(es) accounted for the differences observed in carcinoma mass per rat and estimated tumor growth rate, both the Ki-67 and apoptosis labeling indices were computed. As shown in Table 1, Ki-67 was reduced by 60% ($P < 0.0001$) and the apoptotic index was 129% higher ($P < 0.0001$) in the high versus low n-3 treatment groups (representative photomicrographs in Supplementary Fig. S1). As the next step in analysis, levels of key proteins that regulate the G_1–S transition in the cell cycle and the induction of apoptosis were assessed. The levels of cyclin-D1 and phospho-Rb were reduced and levels of 2 cyclin-dependent kinase inhibitors, p21 and p27, were elevated in the high versus low n-3:n-6 treatment group suggestive of a block in cell-cycle transit at the G_1–S transition (Table 1; representative Western blot analyses in Supplementary Fig. S2A). Relative to apoptosis and consistent with the elevated apoptotic index observed in the high n-3:n-6 group, the level of cleaved PARP (PARP89/116 ratio) was elevated as were levels of Bax and Apaf-1, whereas the level of Bcl-2 was not significantly affected. These changes are indicative of the induction of apoptosis via the intrinsic pathway (Table 1; representative Western blot analyses in Supplementary Fig. S2B).

The processes of cell proliferation and apoptosis are generally linked and consequently changes in regulatory mechanisms can be highly correlated. Moreover, the standard manner of reporting data can mask the ability to visualize differences among the responses of animals within a treatment group as well as the occurrence of overlapping responses between treatment groups. To better understand the proliferative and apoptotic response in this regard, the data were subjected to unsupervised cluster analysis via PCA and to supervised cluster analysis via OPLS-DA, as described in Materials and Methods. As shown in Fig. 1A and B, 100% of the carcinomas were correctly identified with low and high n-3:n-6 group assignment, and the degree of heterogeneity among responses within both groups is shown in the dendrogram that is Fig. 1C. More heterogeneity in response is apparent in the low versus high n-3:n-6 group. Figure 1D shows the 95% CIs for covariance of the 7 proteins evaluated in the first PC sorted in ascending order, which relegates target proteins with elevated expression in the low n-3:n-6 group compared with the high n-3:n-6 group to the distal end of the *x*-axis. These jack-knifed CIs (JKCI) identified proteins with high reliability (green bars) versus low reliability (red bars) as shown in Fig. 1E. Proteins with low reliability, based on error bars crossing 0 provide no useful information relative to identifying the treatment group from

Table 1. Effect of dietary n-3:n-6 ratio on cellular processes regulating cell proliferation and apoptosis

Dietary n-3:n-6 ratio	Low	High	*P*
	0.6	14.6	
Cell proliferation			
Ki-67 index (%)	34.9 ± 1.6	14.0 ± 0.9	<0.0001
Rb^{Ser780} ratio	0.41 ± 0.03	0.26 ± 0.02	<0.0001
Cyclin-D1	1,302 ± 29	967 ± 29	<0.0001
p21	465 ± 31	664 ± 40	0.001
p27	326 ± 11	393 ± 10	<0.0001
Apoptosis			
Apoptotic index (%)	1.71 ± 0.05	3.92 ± 0.13	<0.0001
Bax	188 ± 8	242 ± 9	<0.0001
Bcl-2	589 ± 28	527 ± 26	0.117
Bax/Bcl-2	0.32 ± 0.01	0.47 ± 0.02	<0.0001
Apaf-1	392 ± 9	457 ± 17	0.005
PARP89	795 ± 26	577 ± 53	0.002
PARP116	547 ± 15	292 ± 28	<0.0001
PARP89/116 ratio	1.45 ± 0.02	1.99 ± 0.02	<0.0001

NOTE: Values are means ± SEM (n = 11). The methods for determining the Ki-67 and apoptotic index are described under Materials and Methods. The resulting count data were evaluated by the Kruskal–Wallis rank test. Actin-normalized Western blotting data, which are semiquantitative estimates of protein expression, were analyzed by Kruskal–Wallis rank test. Ratio is the ratio of phospho-protein (arbitrary units of optical density) to non-phospho-protein (arbitrary units of optical density)
Abbreviations: Bax, Bcl-associated X; Bcl, B-cell leukemia oncogene.

which a carcinoma was obtained. Figure 1F shows the ranked importance of proteins and clearly indicated that the proteins contributing most to the classification of carcinomas were associated with the cell-cycle regulation.

Transcription factors

The n-3:n-6 ratio has been reported to affect gene expression by mechanisms dependent on and independent of binding to fatty acid–binding proteins. Given that a considerable body of evidence indicates that n-3 fatty acids mediate effects on cell signaling via binding to PPARα, β/δ, and γ, an initial set of Western blot analyses was conducted to determine levels of each receptor in carcinomas. As shown in Table 2, PPARγ content was increased by 31% in the high versus low n-3 treatment group ($P < 0.001$), whereas the level of β/δ was 14.6% lower ($P = 0.015$) and PPARα was unaffected (representative Western blot analyses are shown in Supplementary Fig. S3). Another family of cell surface receptors that can activate gene expression following fatty acid binding are G-protein–coupled receptors. One such protein, GRP120, is generally associated with macrophages, which was of interest as macrophage invasion of tumors is common. The level of GRP120 was elevated by 18% in carcinomas ($P = 0.001$) from rats fed the high n-3:n-6 ratio.

Because the n-3:n-6 ratio has also been reported to affect transcriptional activity related to inflammation, intermediary metabolism, and cell fate, effects on additional transcriptional factors were assessed, that is, the content of phospho-NF-κB $p65^{Ser536}$, phospho-FOXO-1^{Thr24}, phospho-FOXO-3a ^{Thr32,} Hif-1α, and SIRT-1 were assessed. As shown in Table 2, NF-κβ $p65^{Ser536}$ was 39% lower ($P = 0.001$) and FOXO-1^{Thr24} and FOXO-$3a^{Thr32}$ were 46.5% ($P = 0.001$) and 32.7% ($P < 0.001$) lower, Hif-1α was 32.3% ($P = 0.026$) lower but SIRT-1 was unaffected (21.8% lower, $P = 0.324$) in the high versus low n-3:n-6 treatment groups (representative Western blot analyses are shown in Supplementary Fig. S3). Consistent with the FOXO data, a downstream product associated with FOXO-mediated transcription, GADD153, was 46.5% higher in the high versus low n-3:n-6 treatment group.

To determine the extent to which these changes in protein concentration could correctly classify tumors according to treatment group, data were subjected to PCA and OPLS-DA. As shown in Supplementary Fig. S4, PCA correctly classified 20 of 22 carcinomas, although there was considerable within-group variability in the response pattern. The OPLA-DA analysis, which separates variance associated with treatment group from systematic variation and noise, correctly classified 100% of the carcinomas according to treatment group. The variable with the greatest influence in correct classification was PPARγ (overexpression being negatively associated with carcinoma growth), whereas, phosphorylated FOXO-3a had the greatest influence in identifying carcinomas from the low n-3:n-6 treatment group (positively associated with carcinoma growth).

Growth factor–related signaling

The evaluation of insulin-related signaling involved a large number of proteins in the Akt-mTOR-AMPK–regulated network. As shown in Table 2 (representative Western blot analyses in Supplementary Fig. S5), signaling that is associated

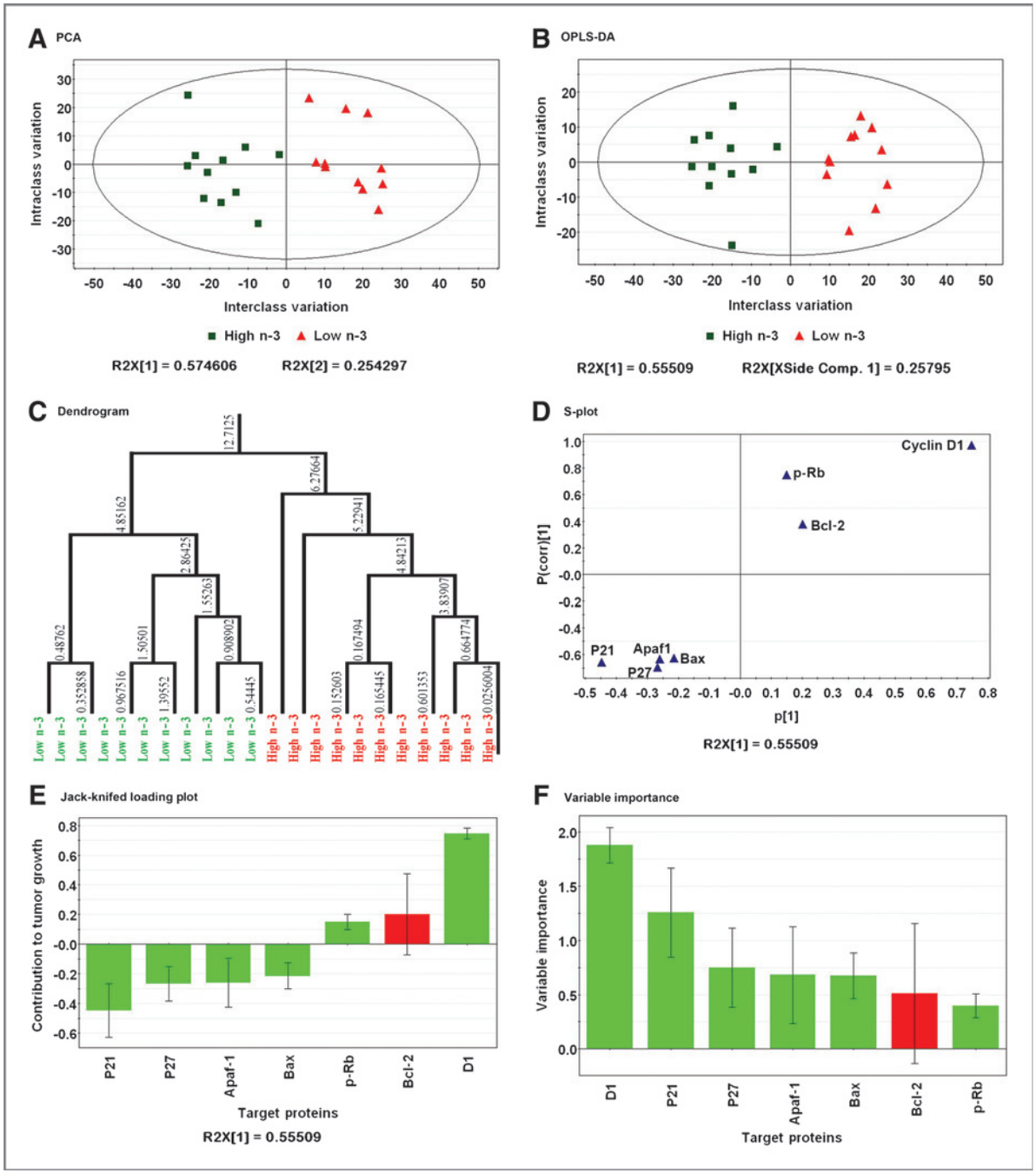

Figure 1. Multivariate discriminant analysis of the actin-normalized intensities for each protein in cell cycle and apoptosis that was Western blotted was used to examine the correlation structure among proteins and distinguish carcinomas based on the treatment group from which they were obtained (low n-3:n-6 or high n-3:n-6). Each point represents an individual carcinoma. A, to visualize inherent clustering patterns, the score scatter plot shows the first 2 score vectors of the PCA model that accounts for 82.9% of the variability in protein expression. No observations lie outside the 95% confidence ellipse. B, OPLS-DA was used to fit a 2-class supervised model and partition the sources of variation. The scatter plot shows the first predictive and first orthogonal components. Complete separation of the carcinomas from each treatment group was observed, and the wide scatter of carcinomas within treatment group along the *y*-axis indicates high within-class variation. C, to visualize the misclassification rate, the dendrogram depicts hierarchical clustering patterns among carcinomas within a treatment group. Node height of cluster 6.27 from 0 confirms the elevated diversity seen within high n-3:n-6 treatment group. To determine the proteins responsible for distinctness of carcinomas in the 2 treatment groups, the OPLS-DA model was reparameterized to compare all low n-3:n-6 carcinomas with all high n-3:n-6 carcinomas. D, the S-plot shows the relationship between the modeled correlation (vertical axis) and the modeled covariance (horizontal axis) from the 2-class OPLS-DA model. Top right and bottom left regions of S-plots contain candidate biomarkers with both high reliability and high magnitude. E, to determine the statistical reliability of the proteins identified as influential in D, JKCIs were estimated for the first predictive component for the proteins evaluated and were sorted in ascending order on the basis of expression in the low n-3:n-6 (control) group; target proteins with JKCI including 0 were indicated by red bars, because they are unreliable predictors of treatment group assignment. F, rank of importance in target proteins.

Table 2. Effect of dietary n-3:n-6 ratio on cellular processes regulating cell transcription factors and insulin signaling

Dietary n-3	Low	High	*P*
Transcription factors			
PPARα	84 ± 12	83 ± 14	0.980
PPARβ	446 ± 19	381 ± 15	0.015
PPARγ	1,212 ± 42	1,589 ± 62	<0.0001
GPR120	282 ± 4	333 ± 5	0.001
NF-κB $p65^{Ser536}$ ratio	5.2 ± 0.4	3.2 ± 0.3	0.001
$FOXO1^{Thr24}$ ratio	0.71 ± 0.07	0.38 ± 0.01	0.001
$FOXO3a^{Thr32}$ ratio	0.52 ± 0.03	0.35 ± 0.02	<0.0001
Hif-1α	799 ± 60	541 ± 88	0.026
SIRT-1	55 ± 7	43 ± 9	0.324
GADD153	71 ± 4	104 ± 5	<0.0001
Growth factor signaling			
IGF-1R	712 ± 56	561 ± 37	0.039
PI3Kp110	106 ± 5	85 ± 4	0.005
$IRS1^{Ser636/639}$ ratio	0.59 ± 0.01	0.47 ± 0.02	<0.0001
$AMPK^{Thr172}$ ratio	0.031 ± 0.001	0.040 ± 0.001	<0.0001
Akt^{Ser473} ratio	0.41 ± 0.01	0.32 ± 0.01	<0.0001
$mTOR^{Ser2448}$ ratio	0.37 ± 0.01	0.31 ± 0.01	0.001
$Raptor^{Ser792}$ ratio	0.032 ± 0.003	0.180 ± 0.008	<0.0001
$PRAS40^{Thr246}$ ratio	1.38 ± 0.02	0.76 ± 0.04	<0.0001
$P70S6K^{Thr389}$ ratio	0.95 ± 0.03	0.74 ± 0.01	<0.0001
$4E\text{-}BP1^{Thr37/46}$ ratio	1.03 ± 0.03	0.76 ± 0.03	<0.0001

NOTE: Values are means ± SEM (n = 11). Ratio is the ratio of phospho-protein (arbitrary units of optical density) to non-phospho-protein (arbitrary units of optical density). Ratio data were analyzed by the Kruskal–Wallis rank test.

Abbreviations: 4E-BP1, eukaryotic translation initiation factor 4E-binding protein 1; Akt, protein kinase B; GADD153, growth arrest and DNA damage protein 153; GPR120, G-protein–coupled receptor 120; PRAS40, 40-kDa proline-rich protein; P70S6K, 70-kDa ribosomal protein S6 kinase; Raptor, regulatory associated protein of mTOR; SIRT-1, sirtuin 1.

with cell proliferation and cell survival was downregulated in high versus low n-3:n-6 treatment group, that is, insulin-like growth factor-1 receptor (IGF-1R; 21.2%; $P = 0.039$), $phospho\text{-}IRS\text{-}1^{Ser636/639}$ (20.3%; $P < 0.0001$), PI3Kp110 (19.8%; $P = 0.005$), AKT (22.0%; $P < 0.0001$), mTOR (16.2%; $P = 0.001$), PRAS40 (44.9%; $P < 0.0001$), P70S6K (22.1%; $P < 0.0001$), and 4E-BP1 (26.2%; $P < 0.0001$), and the arms of the network associated with suppression of mTOR signaling were induced, that is, AMP-activated protein kinase (AMPK; 1.3-fold, $P < 0.0001$) and phospho-Raptor (5.6-fold, $P < 0.0001$). To determine the extent to which these changes in protein concentration could correctly classify tumors according to treatment group, data were subjected to PCA and OPLS-DA. As shown in Supplementary Fig. S6, 19 of 22 carcinomas were correctly classified, there were no carcinomas that were outliers, but there was considerable within-group variability in the response pattern. The OPLS-DA analysis correctly classified 100% of the carcinomas according to treatment group. The variable with the greatest effect in correct classification was phosphorylated P70S6K, whereas IGF-1Rα had the greatest influence in identifying carcinomas from the low n-3:n-6 treatment group (positively associated with carcinoma growth), and phosphorylated AMPK had the greatest influence in identifying carcinomas from the high n-3:n-6 treatment group (negatively associated with carcinoma growth).

Lipid metabolism

In view of these findings, key regulatory points in lipid metabolism were assessed. As shown in Table 3, evidence of significantly decreased lipid biosynthesis [fatty acid synthase (FASN), 20.0% lower, $P < 0.0001$; HMGCR 13.2% lower, $P = 0.001$; SREBP-1 (precursor form) 27.5% lower, $P < 0.0001$] and significantly increased phospho-ACC (1.3-fold, $P < 0.0001$) were observed in the high versus low n-3:n-6 treatment group (representative Western blot analyses shown in Supplementary Fig. S7). As shown in Supplementary Fig. S8, all carcinomas were correctly classified by unsupervised PCA and supervised OPLS-DA cluster analysis. The variable with the greatest effect in correct classification was FASN, which had the greatest influence, and overexpression was positively associated with carcinoma growth, whereas phospho-ACC had the greatest influence in identifying carcinomas from the high n-3:n-6 treatment group (negatively associated with carcinoma growth).

To take advantage of the analytic power of OPLS-DA, one additional analysis was conducted. As shown in Fig. 2, all

Table 3. Effect of dietary n-3:n-6 ratio on proteins regulating lipid metabolism

Dietary n-3	Low	High	*P*
ACC^{Ser79} ratio	2.35 ± 0.13	3.12 ± 0.08	<0.0001
FASN	1,714 ± 39	1,372 ± 34	<0.0001
HMGCR	859 ± 25	746 ± 16	0.001
SREBP-1	385 ± 12	279 ± 5	<0.0001

NOTE: Values are means ± SEM ($n = 11$). Actin-normalized Western blot analysis data, which are semiquantitative estimates of protein expression, and the ratio data were analyzed by Kruskal–Wallis rank test. Ratio is the ratio of phospho-protein (arbitrary units of optical density) to non-phospho-protein (arbitrary units of optical density).

Abbreviations: ACC, acetyl-CoA carboxylase; HMGCR, 3-hydroxy-3-methyl-glutaryl-CoA reductase; SREBP-1, sterol regulatory element-binding protein 1.

signaling proteins were included in the OPLS-DA model statement. Twenty-one of 22 carcinomas were correctly classified by PCA (Fig. 2A). The OPLS-DA analysis correctly classified 100% of the carcinomas according to treatment group (Fig. 2B). The degree of heterogeneity among responses within both groups is shown in the dendrogram that is Fig. 2C. Elevated PPARγ expression was most important to identifying carcinomas in the high n-3:n-6 treatment group (negatively associated with carcinoma growth; Fig. 2D and E), whereas overexpression of FASN was most important to identifying carcinomas in the low n-3:n-6 treatment group (positively associated with carcinoma growth). The variable with the greatest effect in correct classification was FASN (Fig. 2F).

Discussion

Recent evaluations of the literature on the effects of n-3 fatty acids in the prevention and control of breast cancer have provided a mixed view with evidence indicating inhibition, no effect, and enhancement of carcinogenesis (7, 22, 23). In our review (22), a series of recommendations were made concerning the experimental approaches that would serve to guide the design of experiments with the potential of resolving the fish oil–breast cancer conundrum. In pursuit of that objective, our laboratories recently reported a series of experiments in which the dietary ratio of n-3 to n-6 fatty acids varied across a wide range to identify the critical chemistry underlying protection against breast cancer and to define mechanisms associated with inhibition of various aspects of the carcinogenic process without limiting the experimental design by levels of intake currently achievable by the dietary consumption of fish or fish oil supplements (1). It was observed that experimentally verified dietary n-3 to n-6 ratios of 4.9 and 14.6 rendered protection against chemically induced rat mammary cancer in the presence or absence of treatment with tamoxifen. Dietary ratios of n-3 to n-6 less than 4.9 had no effect. Analysis of plasma from treated animals indicated that host systemic factors associated with adipocyte function (leptin and adiponectin) and with growth factor availability homeostasis (IGF-1) were affected by dietary n-3 to n-6 ratios in excess of 4.9. These systemic factors have been implicated in various aspects of breast carcinogenesis, suggesting a potential role in mediating protection (1, 24–26).

Host systemic factors clearly exert effects on the heterogeneous collection of diseases referred to as breast cancer (27). During the process of cellular transformation and the progression of transformed cells to invasive and metastatic stages of cancer, the regulation of cell signaling pathways that is normally subject to interactions with neighboring cells in the tissue and to blood- and lymph-borne systemic factors becomes increasingly independent of those factors, that is, regulation becomes autonomous (28). Thus, the signaling pathways deregulated within carcinomas provide clues about etiology as well as valuable information about potential targets for cancer prevention and control.

The expression of the Ki-67 protein is strictly associated with cell proliferation being present during all active phases of the cell cycle, G_1, S, G_2, and mitosis but absent from resting cells in G_0. This makes Ki-67 an excellent marker for determining growth fraction, that is, the proportion of cells not in G_0, for a given cell population (29). As shown in Table 1, the growth fraction was significantly reduced in the high n-3:n-6 group, and it appeared that this was accompanied by a partial block in cell-cycle progression at the G_1–S transition. As reviewed in the work of Peters and colleagues (7) and Foti and colleagues (10), n-3 fatty acids have been reported to mediate effects on cell proliferation by repressing cyclin-D1 and inducing p21. Strikingly, as shown in Fig. 1, the nonbiased assessment of effects on cellular machinery involved in proliferation and apoptosis identified the effects on cyclin-D1 and p21 as the most influential in distinguishing carcinomas obtained from either the low or high n-3:n-6 treatment groups. While the level of apoptosis was also significantly induced in the high n-3:n-6 group, the analyses shown in Fig. 1 did not identify factors in the apoptotic pathway as exerting a strong effect in identifying the treatment group from which the carcinomas were obtained, a finding suggestive of a dominant effect of n-3 fatty acids on the proliferative machinery of the cell (30).

A large body of literature indicates that n-3 fatty acids exert biologic effects, in part, via the activation of PPAR receptors, which regulate transcription of genes involved in cell proliferation and survival and cellular metabolism (7). The PPAR family of genes codes for α, β/δ, and γ isoforms of receptors. As shown in Table 2, PPARγ was the dominant form of the protein in mammary carcinomas and was increased in carcinomas of

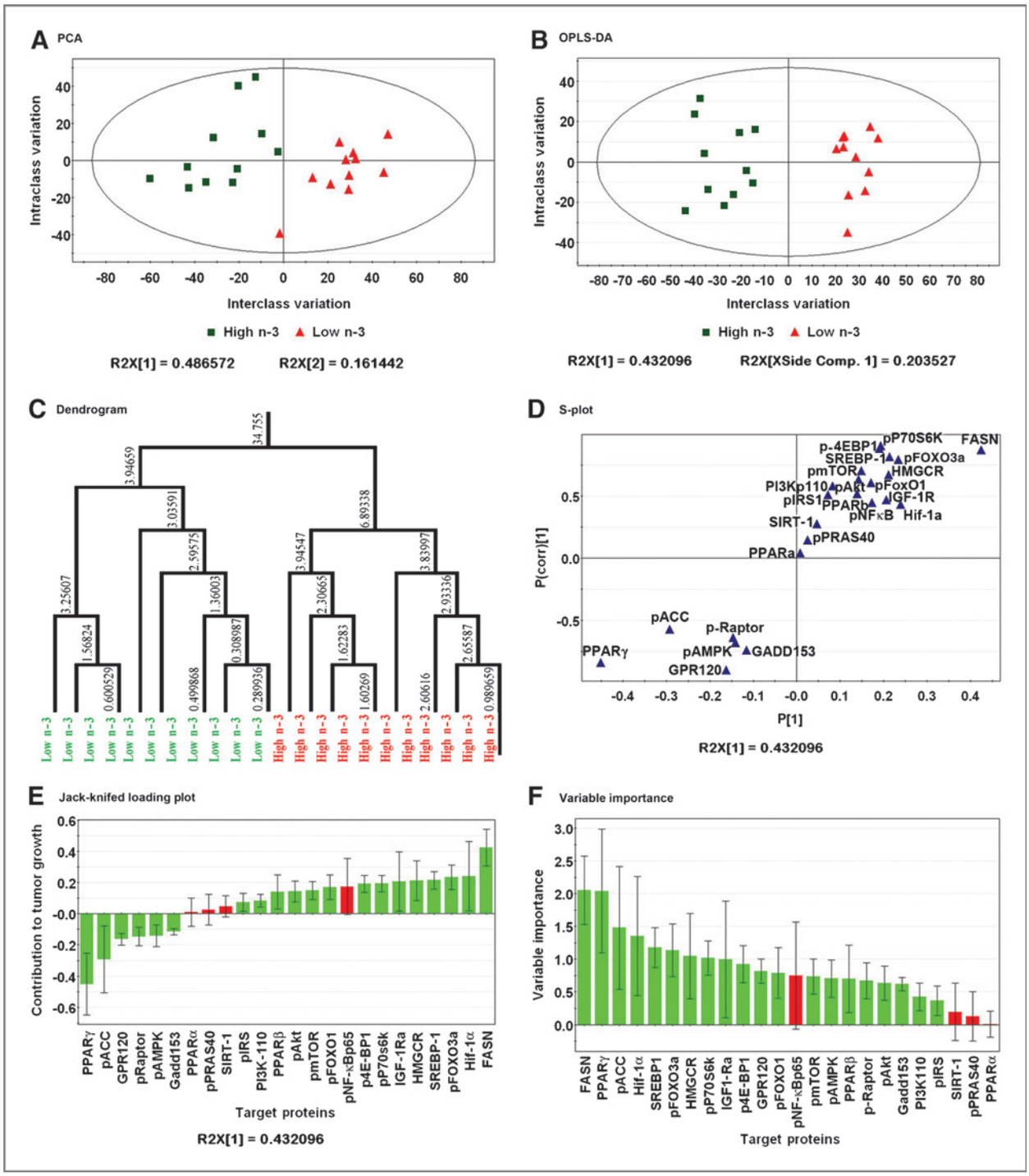

Figure 2. Multivariate discriminant analysis of the actin-normalized intensities for each protein in cellular signaling network that was Western blotted was used to examine the correlation structure among proteins and distinguish carcinomas based on the treatment group from which they were obtained (low n-3:n-6 or high n-3:n-6. Each point represents an individual carcinoma. A, to visualize inherent clustering patterns, the score scatter plot shows the first 2 score vectors of the PCA model that accounts for 64.8% of the variability in protein expression. No observations lie outside the 95% confidence ellipse. B, OPLS-DA was used to fit a 2-class supervised model and partition the sources of variation. The scatter plot shows the first predictive and first orthogonal components. Complete separation of the carcinomas from each treatment group was observed, and the wide scatter of carcinomas within treatment group along the *y*-axis indicates high within-class variation. C, to visualize the misclassification rate, the dendrogram depicts hierarchical clustering patterns among carcinomas within a treatment group. Node height of cluster 6.89 from 0 confirms the elevated diversity seen within high n-3:n-6 treatment group. To determine the proteins responsible for distinctness of carcinomas in the 2 treatment groups, the OPLS-DA model was reparameterized to compare all

the high n-3:n-6 treatment group. This finding is consistent with evidence that the γ-receptor plays a primary role (31) in breast carcinogenesis, as its activation has been a target of drug development for use in cancer prevention and control. While level of protein does not indicate its activation state, canonical patterns of pathway activity associated with PPAR activation were observed in the high n-3:n-6 group, including NF-κB phosphorylation consistent with reduced inflammation (32), reduced phosphorylation of FOXO-1, and at sites consistent with its transcriptional activation, and the elevated level of GADD153, associated with the transcriptional activity of FOXO, observed in the carcinomas from the high n-3:n-6 treatment group (33). Hypoxia-inducible factor (Hif)-1α has also been reported to be co-regulated when PPAR is activated, and the level of this protein was reduced in the carcinomas from the high n-3:n-6 group (34, 35). Thus, in aggregate, the data shown in Table 2 provide a strong case for future investigations that focus on transcriptional activation as a mechanism of interest in elucidating how the n-3:n-6 ratio inhibits tumor growth.

PPARs are 1 of the 4 components of the intracellular energy sensing apparatus, and these receptor proteins monitor fatty acid concentrations and respond to extracellular changes by regulating cellular metabolism, particularly, lipid synthesis and degradation (6, 36). There are many facets to lipid regulation, several of which integrate with other extracellular signals such as insulin and IGF-1 as well as the intracellular energy charge that is monitored by AMPK (37). Given that an inverse association has been reported between plasma IGF-1 and the dietary n-3:n-6 ratio in our previous report (1), an extensive analysis was conducted on components of the AMPK/mTOR/Akt network that is deregulated in the majority of human breast cancers and in the MNU-induced mammary carcinogenesis model (38, 39). As shown in Table 2, conclusive evidence was obtained that mTOR activity was downregulated at multiple nodes in the network in the carcinomas from the high n-3:n-6 dietary group. Of particular interest was the lower levels of IGF-1R and of activated IRS-1 in the high n-3:n-6 group, effects that were reported to be independent of PPAR-mediated transcriptional activity (10). Other noteworthy observations include the activation of AMPK that could be associated with higher levels of plasma adiponectin that we have observed in the high n-3:n-6 group (1), a concomitant phosphorylation of raptor, which is a substrate of AMPK and that is associated with reduced mTOR activity (40–42), a decrease in the phosphorylation of Akt and its substrate PRAS40, which are associated with reduced mTOR activity (42), and decreased levels of phosphorylated p70S6K and 4E-BP1, which are substrates of mTOR and that regulate cell proliferation and cell survival as well as other aspects of cellular metabolism (40). Thus, these data are consistent with the effects of the high n-3:n-6 diet on Ki-67 staining and apoptosis shown in Table 1. Whether they are attributed specifically to altered patterns of gene transcription mediated by PPAR activation, to activation of other fatty acid receptors, to non-canonical effects of fatty acid bound to their cognate receptors, or to changes in eicosanoid metabolism will require additional investigation.

Given the predicted effects of PPARγ activation on lipid metabolism and the established effects of both AMPK and mTOR on lipid metabolism, key regulators of lipid synthesis were assessed (43). As shown in Table 3, the level of phosphorylated ACC was increased in the high n-3:n-6 group, consistent with decreased activity of the enzyme and reduced lipid biosynthesis. Similarly, levels of FASN, HMGCR, and SREBP-1 were reduced, effects consistent with both PPAR activation and reduced mTOR activity (44–50). Strikingly, the unbiased ranking of effects reported in Fig. 2 indicates that alterations in lipid metabolism that are reflected by the levels of the proteins involved in lipid synthesis were the most influential determinants in the 100% correct classification of carcinomas by treatment group by an unsupervised clustering technique. These relationships are illustrated in Fig. 3. The importance of *de novo* lipid biosynthesis as a limiting factor for tumor growth is receiving increasing attention (51), and the potential role of the n-3 to n-6 ratio in limiting intratumoral lipid biosynthesis merits scrutiny. Nonetheless, both measures of enzyme activity of proteins involved in lipid synthesis and GC- or liquid chromatography-time-of flight-MS of tissue lipid profiles are required to confirm effects on the biosynthetic process.

Heterogeneity of response

A novel aspect of the data analyses used herein was the application of supervised and unsupervised clustering techniques in an effort to minimize interpretation bias and to characterize the heterogeneity of responses observed both within and between treatment groups. The use of the unsupervised PCA method, shown in Figs. 1A and 2A and Supplementary Figs. S4, S6, and S8, shows the extent of overlap in response between treatment groups for each category into which we divided the proteins that were evaluated, recognizing that some proteins could be listed in more than one category. Such overlap between groups, while embedded in mean and SE statistics, can easily be overlooked in data interpretation, which the graphic analysis helps keep in perspective. The supervised clustering approach that we also applied to the data, remaining panels in those figures with test statistics summarized in Supplementary Table S3, has the advantage that it divides the variance in response to the component associated with treatment group, the variance within a treatment group not associated with the treatment, and a final component that is unexplained variance and is frequently viewed as the biologic noise in the system. From the OPLS-DA

low n-3:n-6 carcinomas with all high n-3:n-6 carcinomas. D, the S-plot shows the relationship between the modeled correlation (vertical axis) and the modeled covariance (horizontal axis) from the 2-class OPLS-DA model. Top right and bottom left regions of S-plots contain candidate biomarkers with both high reliability and high magnitude. E, to determine the statistical reliability of the proteins identified as influential in D, JKCIs were estimated for the first predictive component for the proteins evaluated and were sorted in ascending order on the basis of expression in the low n-3:n-6 (control) group; target proteins with JKCI including 0 were indicated by red bars, because they are unreliable predictors of treatment group assignment. F, rank of importance in target proteins.

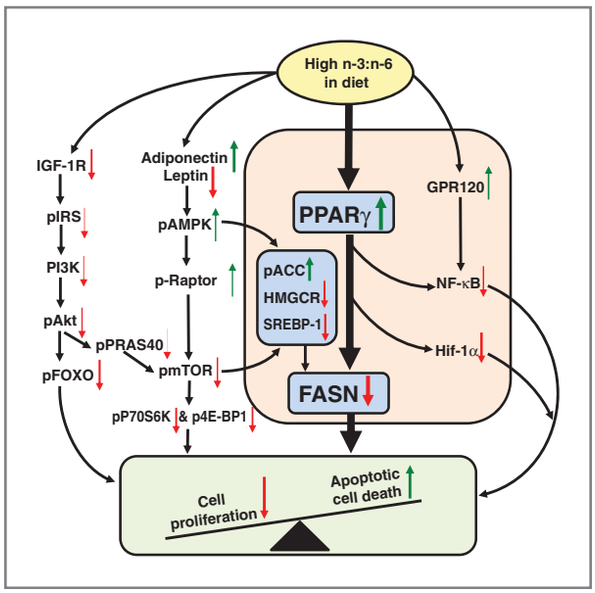

Figure 3. Cellular processes regulating transcription factors, insulin signaling, and lipid synthesis that are likely to account for the effects on cell proliferation and apoptosis in mammary carcinomas of rats fed high versus low (control) dietary ratio of n-3:n-6 fatty acids. Diameter of red (decreased expression) and green arrows (increased expression) indicates magnitude of effect and font size of stated proteins indicates relative importance as determined by OPLS-DA. PPARγ and to a lesser extent, G-protein–coupled protein receptor 120 (GPR120) attenuate inflammation via direct or indirect effects on NF-κB and HIF-1α. PPARγ affects multiple targets in lipid metabolism including FASN. In addition, high dietary n-3:n-6 is accompanied by reduced activity of the mTOR as reflected in the reduced phosphorylation of its downstream targets including 70-kDa ribosomal protein S6 kinase (P70S6K) and eukaryotic translation initiation factor 4E-binding protein 1 (4E-BP1), which in turn, exert effects on cell proliferation and cell survival. Mechanisms by which mTOR activity is downregulated include (i) downregulation of IGF-1R, phosphorylated insulin receptor substrate 1 (pIRS1), phosphoinositide 3-kinase (PI3K), phosphorylated Akt, phosphorylated Forkhead box O, and phosphorylated 40-kDa proline-rich protein (PRAS40) and (ii) upregulation of pAMPK by increased adiponectin and decreased leptin, phosphorylated acetyl-CoA carboxylase (ACC), and phosphorylated regulatory-associated protein of mTOR (Raptor). Decreased phosphorylated mTOR and increased pAMPK further attenuate fatty acids synthesis via reduction of 3-hydroxy-3-methyl-glutaryl-CoA reductase (HMGCR) and of sterol regulatory element-binding protein-1 (SREBP-1) that results in decrease of FASN. The overall consequence of these changes in cell signaling is a decrease in cell proliferation and an increase in cell death by apoptosis.

analyses, B to D of these figures, we observe that (i) there is 100% ability to correctly classify carcinomas when variance is segregated into its variance components, (ii) the effect of treatment is strong, accounting for 45% to 55% of the variance depending on the category of proteins assessed, and (iii) while considerably smaller than the effect of treatment, there is considerable variation in response within groups that we judge is likely to be due to differences among molecular subtypes of mammary cancer induced in this model.

Limitations

Lipid metabolism has 2 important facets, synthesis and degradation, and they are interrelated. While the focus of the analyses reported herein was on synthesis, it is critical that these studies be extended to lipid catabolism. The work reported is also limited in that eicosanoid metabolism was not considered. This is a highly complex topic and will be the subject of a distinct line of investigation that is beyond the scope of the work reported herein.

Summary of potential impact

The evidence presented indicates considerable heterogeneity in the nature of carcinoma responsiveness to n-3 fatty acids indicating a need for assessing how various molecular subtypes of breast cancer respond to an abundance of n-3 relative to n-6 fatty acids in the diet. This information is required to better understand factors that affect cancer risk but even more importantly to understand whether n-3 fatty acids could play a role in the management of various molecular subtypes of the disease. The fact that such a high ratio of dietary n-3:n-6 fatty acids was required to achieve the profound effects on tumor growth reported herein not only indicates that these biologic activities are not likely to be achieved by dietary consumption of fish but also that there are specific metabolites of n-3 fatty acids that account for these effects and that are likely to be endogenously synthesized metabolites, the production of which is normally rate-limited. The rate-limited synthesis of specific n-3 fatty acid metabolites may account, at least in part, for the current conundrum in the n-3 fatty acid, breast cancer literature. The identification of the pentultimate metabolites that account for anticancer activity is made feasible by the exaggeration of the dietary ratios of n-3:n-6 fatty acids as reported herein and is the focus of our ongoing investigations.

Disclosure of Potential Conflicts of Interest

No potential conflicts of interest were disclosed.

Authors' Contributions

Conception and design: W. Jiang, Z. Zhu, A. Manni, H.J. Thompson
Development of methodology: W. Jiang, Z. Zhu, H.J. Thompson
Acquisition of data (provided animals, acquired and managed patients, provided facilities, etc.): W. Jiang, Z. Zhu, J.N. McGinley, H.J. Thompson
Analysis and interpretation of data (e.g., statistical analysis, biostatistics, computational analysis): W. Jiang, Z. Zhu, J.N. McGinley, H.J. Thompson
Writing, review, and/or revision of the manuscript: W. Jiang, Z. Zhu, J.N. McGinley, K. El Bayoumy, A. Manni, H.J. Thompson
Administrative, technical, or material support (i.e., reporting or organizing data, constructing databases): W. Jiang, Z. Zhu, J.N. McGinley, H.J. Thompson
Study supervision: W. Jiang, Z. Zhu, A. Manni, H.J. Thompson

Acknowledgments

The authors thank John Richie and Bogden Prokopczyk who conducted the lipid analyses referenced in this manuscript.

Grant Support

This work was supported by the Susan G. Komen Foundation (KG081632).

The costs of publication of this article were defrayed in part by the payment of page charges. This article must therefore be hereby marked *advertisement* in accordance with 18 U.S.C. Section 1734 solely to indicate this fact.

Received March 19, 2012; revised April 24, 2012; accepted May 10, 2012; published OnlineFirst May 31, 2012.

References

1. Zhu Z, Jiang W, McGinley JN, Prokopczyk B, Richie JP Jr, El BK, et al. Mammary gland density predicts the cancer inhibitory activity of the N-3 to N-6 ratio of dietary fat. Cancer Prev Res (Phila) 2011;4:1675–85.
2. Maclennan M, Ma DW. Role of dietary fatty acids in mammary gland development and breast cancer. Breast Cancer Res 2010;12:211.
3. Thompson HJ, Strange R, Schedin PJ. Apoptosis in the genesis and prevention of cancer. Cancer Epidemiol Biomarkers Prev 1992;1: 597–602.
4. Yee LD, Young DC, Rosol TJ, Vanbuskirk AM, Clinton SK. Dietary (n-3) polyunsaturated fatty acids inhibit HER-2/neu-induced breast cancer in mice independently of the PPARgamma ligand rosiglitazone. J Nutr 2005;135:983–8.
5. Robbins GT, Nie D. PPAR gamma, bioactive lipids, and cancer progression. Front Biosci 2012;17:1816–34.
6. Tyagi S, Gupta P, Saini AS, Kaushal C, Sharma S. The peroxisome proliferator-activated receptor: a family of nuclear receptors role in various diseases. J Adv Pharm Technol Res 2011;2:236–40.
7. Peters JM, Shah YM, Gonzalez FJ. The role of peroxisome proliferator-activated receptors in carcinogenesis and chemoprevention. Nat Rev Cancer 2012;12:181–95.
8. Kremmyda LS, Tvrzicka E, Stankova B, Zak A. Fatty acids as biocompounds: their role in human metabolism, health and disease - a review. Part 2: Fatty acid physiological roles and applications in human health and disease. Biomed Pap Med Fac Univ Palacky Olomouc Czech Repub 2011;155:195–218.
9. Wang D, Dubois RN. Eicosanoids and cancer. Nat Rev Cancer 2010;10:181–93.
10. Foti DP, Paonessa F, Chiefari E, Brunetti A. New target genes for the peroxisome proliferator-activated receptor-gamma (PPARgamma) antitumour activity: perspectives from the insulin receptor. PPAR Res 2009;2009:571365.
11. Thompson HJ, McGinley JN, Rothhammer K, Singh M. Rapid induction of mammary intraductal proliferations, ductal carcinoma *in situ* and carcinomas by the injection of sexually immature female rats with 1-methyl-1-nitrosourea. Carcinogenesis 1995;16:2407–11.
12. McGinley JN, Knott KK, Thompson HJ. Effect of fixation and epitope retrieval on BrdU indices in mammary carcinomas. J Histochem Cytochem 2000;48:355–62.
13. Kerr JF, Wyllie AH, Currie AR. Apoptosis: a basic biological phenomenon with wide-ranging implications in tissue kinetics. Br J Cancer 1972;26:239–57.
14. Walker NI, Bennett RE, Kerr JF. Cell death by apoptosis during involution of the lactating breast in mice and rats. Am J Anat 1989;185:19–32.
15. Jiang W, Zhu Z, Thompson HJ. Effect of energy restriction on cell cycle machinery in 1-methyl-1-nitrosourea-induced mammary carcinomas in rats. Cancer Res 2003;63:1228–34.
16. Snedecor GW, Cochran WG. Statistical methods. 8th ed. Ames, IA: Iowa State University Press; 1989.
17. Morrison DF. Multivariate statistical methods. 3rd ed. New York: McGraw-Hill Publishing Co.; 1990.
18. Gabrielsson J, Jonsson H, Airiau C, Schmidt B, Escott R, Trygg J. OPLS methodology for analysis of pre-processing effects on spectroscopic data. Chemom Intell Lab Syst 2006;84:153–8.
19. Wiklund S, Johansson E, Sjostrom L, Mellerowicz EJ, Edlund U, Shockcor JP, et al. Visualization of GC/TOF-MS-based metabolomics data for identification of biochemically interesting compounds using OPLS class models. Anal Chem 2008;80:115–22.
20. Trygg J, Wold S. Orthogonal projections to latent structures (O-PLS). J Chemom 2002;16:119–28.
21. Wiklund S. Multivariate data analysis and modeling in "omics". Umeå, Sweden: Umetrics; 2008.
22. Signori C, El-Bayoumy K, Russo J, Thompson HJ, Richie JP, Hartman TJ, et al. Chemoprevention of breast cancer by fish oil in preclinical models: trials and tribulations. Cancer Res 2011;71:6091–6.
23. Heinze VM, Actis AB. Dietary conjugated linoleic acid and long-chain n-3 fatty acids in mammary and prostate cancer protection: a review. Int J Food Sci Nutr 2011;63:66–78.
24. Pollak M. Insulin-like growth factor-related signaling and cancer development. Recent Results Cancer Res 2007;174:49–53.
25. Grossmann ME, Ray A, Nkhata KJ, Malakhov DA, Rogozina OP, Dogan S, et al. Obesity and breast cancer: status of leptin and adiponectin in pathological processes. Cancer Metastasis Rev 2010;29:641–53.
26. Ray A, Cleary MP. Leptin as a potential therapeutic target for breast cancer prevention and treatment. Expert Opin Ther Targets 2010;14: 443–51.
27. Goodwin PJ. Host-related factors in breast cancer: an underappreciated piece of the puzzle? J Clin Oncol 2008;26:3299–300.
28. Hanahan D, Weinberg RA. The hallmarks of cancer. Cell 2000;100: 57–70.
29. Scholzen T, Gerdes J. The Ki-67 protein: from the known and the unknown. J Cell Physiol 2000;182:311–22.
30. Albino AP, Juan G, Traganos F, Reinhart L, Connolly J, Rose DP, et al. Cell cycle arrest and apoptosis of melanoma cells by docosahexaenoic acid: association with decreased pRb phosphorylation. Cancer Res 2000;60:4139–45.
31. Houston KD, Copland JA, Broaddus RR, Gottardis MM, Fischer SM, Walker CL. Inhibition of proliferation and estrogen receptor signaling by peroxisome proliferator-activated receptor gamma ligands in uterine leiomyoma. Cancer Res 2003;63:1221–7.
32. Martinez-Micaelo N, Gonzalez-Abuin N, Terra X, Richart C, Ardevol A, Pinent M, et al. Omega-3 docosahexaenoic acid and procyanidins inhibit cyclo-oxygenase activity and attenuate NF-kappaB activation through a p105/p50 regulatory mechanism in macrophage inflammation. Biochem J 2012;441:653–63.
33. Kitamura T, Kitamura Y. [The roles of PPAR, C/EBP and FoxO families in adipocyte differentiation and proliferation]. Nihon Rinsho 2011;69 Suppl 1:259–63.
34. Reuter S, Gupta SC, Chaturvedi MM, Aggarwal BB. Oxidative stress, inflammation, and cancer: how are they linked? Free Radic Biol Med 2010;49:1603–16.
35. Kim EH, Surh YJ. 15-deoxy-Delta12,14-prostaglandin J2 as a potential endogenous regulator of redox-sensitive transcription factors. Biochem Pharmacol 2006;72:1516–28.
36. Jeninga EH, Schoonjans K, Auwerx J. Reversible acetylation of PGC-1: connecting energy sensors and effectors to guarantee metabolic flexibility. Oncogene 2010;29:4617–24.
37. Howell JJ, Manning BD. mTOR couples cellular nutrient sensing to organismal metabolic homeostasis. Trends Endocrinol Metab 2011;22:94–102.
38. Thompson MD, Mensack MM, Jiang W, Zhu Z, Lewis MR, McGinley JN, et al. Cell signaling pathways associated with a reduction in mammary cancer burden by dietary common bean (Phaseolus vulgaris L.). Carcinogenesis 2012;33:226–32.
39. Jiang W, Zhu Z, Thompson HJ. Dietary energy restriction modulates the activity of AMP-activated protein kinase, Akt, and mammalian target of rapamycin in mammary carcinomas, mammary gland, and liver. Cancer Res 2008;68:5492–9.
40. Ghayad SE, Cohen PA. Inhibitors of the PI3K/Akt/mTOR pathway: new hope for breast cancer patients. Recent Pat Anticancer Drug Discov 2010;5:29–57.
41. Brown KA, Hunger NI, Docanto M, Simpson ER. Metformin inhibits aromatase expression in human breast adipose stromal cells via stimulation of AMP-activated protein kinase. Breast Cancer Res Treat 2010;123:591–6.
42. Gwinn DM, Shackelford DB, Egan DF, Mihaylova MM, Mery A, Vasquez DS, et al. AMPK phosphorylation of raptor mediates a metabolic checkpoint. Mol Cell 2008;30:214–26.
43. Laplante M, Sabatini DM. An emerging role of mTOR in lipid biosynthesis. Curr Biol 2009;19:R1046–52.
44. Cleary MP, Ray A, Rogozina OP, Dogan S, Grossmann ME. Targeting the adiponectin:leptin ratio for postmenopausal breast cancer prevention. Front Biosci (Schol Ed) 2009;1:329–57.
45. Muhlhausler BS, Cook-Johnson R, James M, Miljkovic D, Duthoit E, Gibson R. Opposing effects of omega-3 and omega-6 long chain polyunsaturated Fatty acids on the expression of lipogenic genes in omental and retroperitoneal adipose depots in the rat. J Nutr Metab 2010;2010.pii: 927836.

46. Menendez JA, Mehmi I, Atlas E, Colomer R, Lupu R. Novel signaling molecules implicated in tumor-associated fatty acid synthase-dependent breast cancer cell proliferation and survival: Role of exogenous dietary fatty acids, p53-p21WAF1/CIP1, ERK1/2 MAPK, p27KIP1, BRCA1, and NF-kappaB. Int J Oncol 2004;24:591–608.
47. Howell G III, Deng X, Yellaturu C, Park EA, Wilcox HG, Raghow R, et al. N-3 polyunsaturated fatty acids suppress insulin-induced SREBP-1c transcription via reduced trans-activating capacity of LXRalpha. Biochim Biophys Acta 2009;1791:1190–6.
48. Guntur KV, Guilherme A, Xue L, Chawla A, Czech MP. Map4k4 negatively regulates peroxisome proliferator-activated receptor (PPAR) gamma protein translation by suppressing the mammalian target of rapamycin (mTOR) signaling pathway in cultured adipocytes. J Biol Chem 2010;285:6595–603.
49. Kaur G, Sinclair AJ, Cameron-Smith D, Barr DP, Molero-Navajas JC, Konstantopoulos N. Docosapentaenoic acid (22:5n-3) down-regulates the expression of genes involved in fat synthesis in liver cells. Prostaglandins Leukot Essent Fatty Acids 2011;85:155–61.
50. Lu J, Borthwick F, Hassanali Z, Wang Y, Mangat R, Ruth M, et al. Chronic dietary n-3 PUFA intervention improves dyslipidaemia and subsequent cardiovascular complications in the JCR:LA- cp rat model of the metabolic syndrome. Br J Nutr 2011;105:1572–82.
51. Jones RG, Thompson CB. Tumor suppressors and cell metabolism: a recipe for cancer growth. Genes Dev 2009;23:537–48.